Carbohydrate Research 343 (2008) 2947–2955

Contents lists available at ScienceDirect

Carbohydrate Research

journal homepage: www.elsevier.com/locate/carres

# A basidiomycetous yeast, *Pseudozyma crassa*, produces novel diastereomers of conventional mannosylerythritol lipids as glycolipid biosurfactants

Tokuma Fukuoka [a], Mayo Kawamura [b], Tomotake Morita [a], Tomohiro Imura [a], Hideki Sakai [b], Masahiko Abe [b], Dai Kitamoto [a,*]

[a] *Research Institute for Innovation in Sustainable Chemistry, National Institute of Advanced Industrial Science and Technology (AIST), Tsukuba Central 5-2, 1-1-1, Higashi, Tsukuba, Ibaraki 305-8565, Japan*
[b] *Faculty of Science and Technology, Tokyo University of Science, Yamazaki 2641, Noda, Chiba 278-8510, Japan*

ARTICLE INFO

*Article history:*
Received 22 July 2008
Received in revised form 25 August 2008
Accepted 31 August 2008
Available online 9 September 2008

*Keywords:*
Biosurfactant
Glycolipid
Mannosylerythritol lipid
Erythritol
*Pseudozyma crassa*
*Pseudozyma* yeasts

ABSTRACT

Mannosylerythritol lipids (MELs) are glycolipid biosurfactants produced by the yeast strains of the genus *Pseudozyma*. These compounds show not only excellent surface-active properties, but also versatile biochemical actions. During a survey of new MEL producers, we found that a basidiomycetous yeast, *Pseudozyma crassa*, extracellularly produces three glycolipids. When glucose and oleic acid were used as the carbon source, the total amount of glycolipids reached approximately 4.6 g/L in the culture medium. The structures of these glycolipids were similar to those of well-known MEL-A, -B, and -C, respectively. Very interestingly, in all the present glycolipids, the configuration of the erythritol moiety was entirely opposite to that of conventional MELs. The present glycolipids were identified to have the carbohydrate structure of 4-*O*-β-D-mannopyranosyl-(2*R*,3*S*)-erythritol, stereochemically different from 4-*O*-β-D-mannopyranosyl-(2*S*,3*R*)-erythritol of conventional MELs. Furthermore, these new glycolipids possessed both short-chain acids ($C_2$ or $C_4$) and long-chain acids ($C_{14}$, $C_{16}$, or $C_{18}$) on the mannose moiety. The major component of the present glycolipids clearly showed different interfacial and biological properties, compared to conventional MELs comprising two medium-chain acids on the mannose moiety. Accordingly, the novel MEL diastereomers produced by *P. crassa* should provide us with different glycolipid functions, and facilitate a broad range of applications of MELs.



## 1. Introduction

Mannosylerythritol lipids (MELs, Fig. 1) are one of the most promising biosurfactants,[1–3] which are amphiphilic compounds abundantly produced by different microorganisms from renewable resources. MELs are produced in large amounts (over 100 g/L) from different vegetable oils by yeast strains belonging to the genus *Pseudozyma*.[4–6] These glycolipids exhibit not only excellent surface-active properties,[7] but also versatile biochemical actions,[2,8–14] including cell-differentiation induction of different mammalian cells[11] as well as affinity binding toward different immunoglobulins.[8,13,14] Moreover, MELs markedly increase the efficiency of gene transfection mediated by cationic liposomes via membrane fusion between liposomes and plasma membranes.[10,15] MELs have thus great potential not only as environmentally friendly surfactants but also as advanced biomedical materials.

Well-known MELs, namely MEL-A, -B, and -C, have 4-*O*-β-D-mannopyranosyl-(2*S*,3*R*)-erythritol as the hydrophilic part and two fatty acyl groups as the hydrophobic part. In addition, these MEL homologs have one or two acetyl groups at the C-4′ and/or C-6′ in the mannose moiety (Fig. 1). Interestingly, these glycolipids show specific phase behavior and different self-assembled structures in aqueous solutions,[16–20] although the difference in the chemical structure is very small. For instance, MEL-A spontaneously forms an $L_3$ (sponge) phase in a wide range

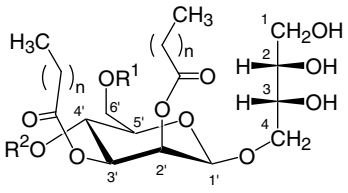


**Figure 1.** Chemical structures of the conventional mannosylerythritol lipids.

* Corresponding author. Tel.: +81 29 861 4664; fax: +81 29 861 4660.
*E-mail address:* dai-kitamoto@aist.go.jp (D. Kitamoto).

0008-6215/$ - see front matter © 2008 Elsevier Ltd. All rights reserved.
doi:10.1016/j.carres.2008.08.034

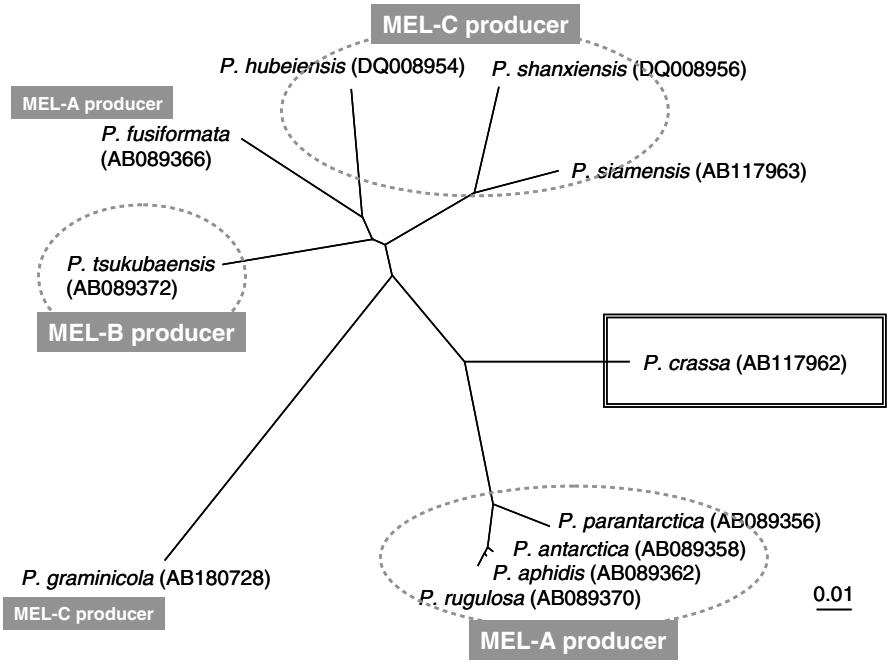


**Figure 2.** Molecular phylogenetic tree constructed using ITS1, 5.8S rDNA gene, and ITS2 sequences of the genus *Pseudozyma*. The DDBJ/GenBank/EMBL accession numbers are indicated in parentheses.

of concentrations, while MEL-B forms $L_\alpha$ (lamellar) and myelin structures.

In the known high-level MEL producers such as *Pseudozyma antarctica*,[4] *Pseudozyma aphidis*,[5] and *Pseudozyma rugulosa*,[6] MEL-A is produced in the largest amount and comprises more than 70% of the total MELs. On the other hand, we have recently demonstrated that MEL-B and MEL-C are predominantly produced by *Pseudozyma tsukubaensis*[21,22] and *Pseudozyma hubeiensis*,[22,23] respectively. The developments of new producers and structural variety would make a wide range of applications of MELs possible. We have thus focused our attention on the relationship between the production pattern of MELs and the taxonomical characteristics of the producer, and continued to investigate the MEL productivity of different *Pseudozyma* strains (Fig. 2) aiming to develop new MEL producers.

During the course of our study, we found that *Pseudozyma crassa*, which was a recently identified strain of the genus and located at a distance from known MEL producers on the phylogenetic tree, secretes glycolipids with a different behavior on thin-layer chromatography (TLC) compared to conventional MELs (Fig. 3). In this study, we investigated the production conditions of the glycolipids by *P. crassa* and performed their structural characterization. We also addressed the interfacial and biochemical properties of the novel glycolipid biosurfactants.

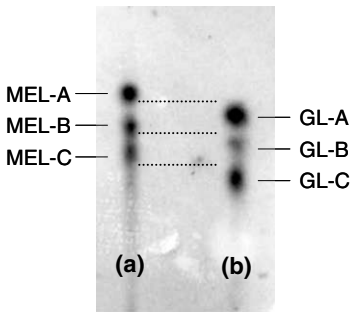


**Figure 3.** TLC pattern of glycolipids produced by (a) *P. antarctica* and (b) *P. crassa*.

## 2. Results

### 2.1. Production of glycolipids by *P. crassa* CBS 9959$^T$

Based on preliminary experiments using a basal medium, *P. crassa* CBS 9959$^T$ was found to secrete a mixture of glycolipids. Interestingly, on TLC, the mixture gave three spots of glycolipids showing different $R_f$ values compared to conventional MEL-A, -B, and -C, which were obtained with *P. antarctica* T-34 (Fig. 3). Hence, we tentatively investigated the glycolipid production conditions, so as to achieve the structural characterization.

In *P. crassa*, the yield of glycolipids clearly increased when fatty acids and carbohydrates were simultaneously used as the carbon source, compared to the case of fatty acids only. As a result of experiments using a jar-fermentor, the best yield was obtained with the fermentation medium containing 4% oleic acid and 4% glucose, and the amount of glycolipids reached approximately 4.6 g/L after seven days of cultivation.

### 2.2. Characterization of the purified glycolipids produced by *P. crassa* CBS 9959$^T$

The produced glycolipids were extracted from the culture medium with ethyl acetate, and purified into three glycolipids, namely GL-A, -B, and -C, by silica gel column chromatography (Fig. 3). Structure determination of the purified glycolipids was then performed by nuclear magnetic resonance (NMR) analyses. The $^1$H NMR spectrum of GL-A (Fig. 4a) showed a similar peak pattern to that of known MEL-A produced by *P. antarctica*. However, when the spectra were compared more in detail, GL-A had different peak patterns in both the carbohydrate moiety and the fatty chain moiety. For example, Figure 4b shows partial $^1$H NMR spectra of the carbohydrate moiety of GL-A and conventional MEL-A. The two resonances arising from the H-4a and H-4b in the erythritol (~3.8–4.1 ppm) were widely separated in the conventional MEL-A, while these peaks overlapped in GL-A. Moreover, there were clear differences in the resonances of the mannose anomeric hydrogen (H-1′) and H-6′ between GL-A and MEL-A.

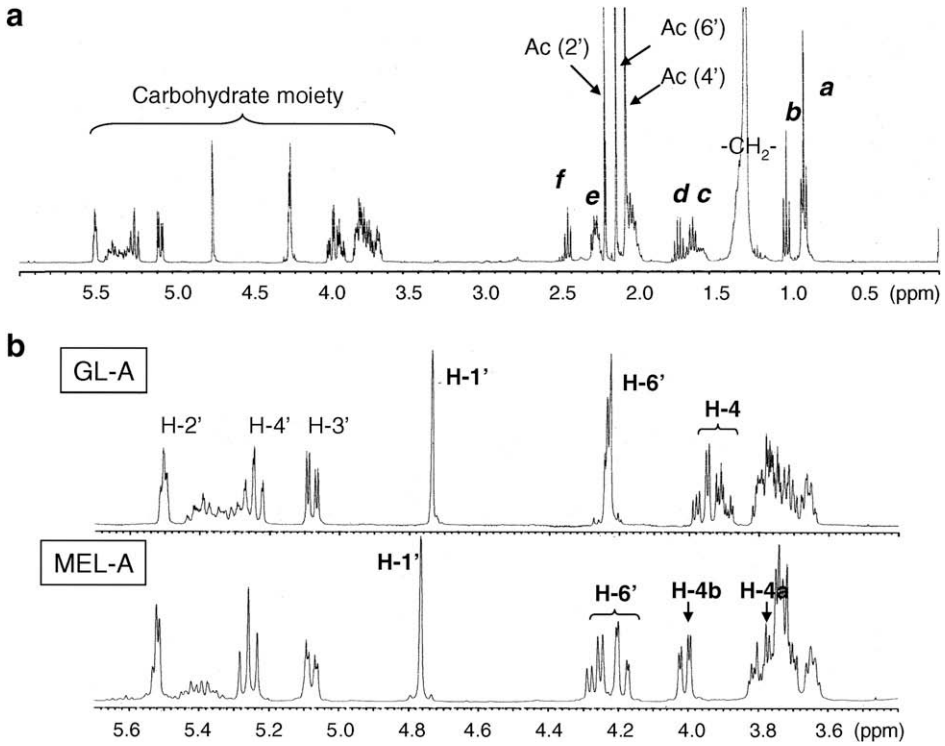


**Figure 4.** (a) $^1$H NMR spectrum of GL-A produced by *P. crassa* (b) Partial $^1$H NMR spectra of GL-A and MEL-A produced by *P. antarctica*.

These differences between GL-A and MEL-A agreed well with those between two MEL-A diastereomers, which was previously synthesized and reported by Crich and co-workers.[24] We recently reported that *P. tsukubaensis* produces a new diastereomer of conventional MEL-B.[25] Interestingly, an $^1$H NMR spectrum of the new diastereomer showed a similar peak pattern to that of GL-B (data not shown). Accordingly, GL-A was estimated to be the diastereomer of conventional MEL-A, and to have 4-*O*-β-D-mannopyranosyl-(2*R*,3*S*)-erythritol as the carbohydrate moiety (Fig. 5).

To confirm the carbohydrate configuration, the carbohydrate moiety, namely mannosylerythritol (ME), was prepared by alkaline hydrolysis from GL-A and compared with that from MEL-A. The purified ME from *P. antarctica* was obtained as a white needle-like crystal by recrystallization from 90% ethanol. Its melting point was 155.4–158.3 °C and the $[\alpha]_D$ value at 27 °C was −35.2 (*c* 1.0, $H_2O$). In contrast, the ME from *P. crassa* was obtained not as a solid but as a colorless syrup. Its $[\alpha]_D$ value at 27 °C was −41.9 (*c* 1.0, $H_2O$). These data for the ME from *P. crassa* were nearly the same as that from *P. tsukubaensis*.[25] Furthermore, the results of NMR analyses of both MEs were also completely consistent with those of the previous study.[25] Consequently, GL-A was identified as the diastereomer of conventional MEL-A.

On the other hand, when paying attention to fatty ester domains at around 0.8–2.5 ppm in the $^1$H NMR spectrum of GL-A (Fig. 4a), it had also distinctly different peak patterns compared to conventional MEL-A. In $^1$H NMR spectrum of MEL-A, broad monomodal peaks at 0.8–1.1 ppm (–$CH_3$) and at 1.5–1.8 ppm (–$CH_3CH_2CO$–) were detected (data not shown). However, in the case of GL-A, Figure 4a shows that these peaks were clearly distinguished by two peaks, which consisted of a sharp one (peak ***b*** and ***d***) and a wide one (***a*** and ***c***), respectively. In addition, there were three sharp peaks at 2.04, 2.10, and 2.18 ppm that were derived from an acetyl group, in spite of the fact that MEL-A has only two acetyl groups at the C-4′ and C-6′ positions (Fig. 1). Then, we tried to confirm the structure in detail by two-dimensional NMR analyses such as $^1$H–$^1$H correlation spectroscopy (COSY), heteronuclear multiple quantum correlation (HMQC), and heteronuclear multiple bond correlation (HMBC).

In the $^1$H–$^1$H COSY spectrum of GL-A (Fig. 6), peak *a* (–$CH_3$) correlated with the broad peak at 1.2–1.4 ppm, which was derived from methylene protons (–$CH_2$–). But the triplet peak *b* (–$CH_3$) correlated with sextet peak *d*. In addition, peak *d* also correlated with triplet peak *f*, which was derived from the proton next to the carbonyl group (–C*H*$_2$CO–) esterified at the C-2′ position of the mannose moiety. The esterified position was assigned by HMBC analysis (data not shown). Meanwhile, peak *c* correlated with the peak *e* (–C*H*$_2$CO– at the C-3′ position) and the broad peak at 1.2–1.4 ppm (–$CH_2$–). As the above results indicate, GL-A was confirmed to have a butanoyl ester at the C-2′ position and a fatty ester at the C-3′ position, respectively.

Furthermore, by HMQC and HMBC analyses, three resonances at 2.04, 2.10, and 2.18 ppm were assigned as the acetyl group at the C-4′, C-6′, and C-2′ positions, respectively (data not shown). GL-A is thus likely to have an acetyl ($C_2$) or butanoyl ($C_4$) group at the C-2′ position. In fact, HMBC spectrum of GL-A demonstrated that H-2′ proton correlated with both resonances at 170.8 and 173.4 ppm, which were derived from carbonyl carbons (C=O) of an acetyl group and butanoyl group, respectively. Incidentally, the relative proportion of acetyl and butanoyl groups was estimated to be 60:40 from the $^1$H NMR spectrum. All NMR data of GL-A are summarized in experimental part.

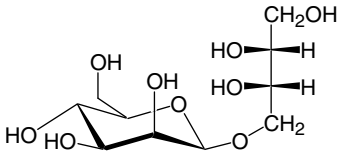


**Figure 5.** The carbohydrate structure of GL-A: 4-*O*-β-D-mannopyranosyl-(2*R*,3*S*)-erythritol.

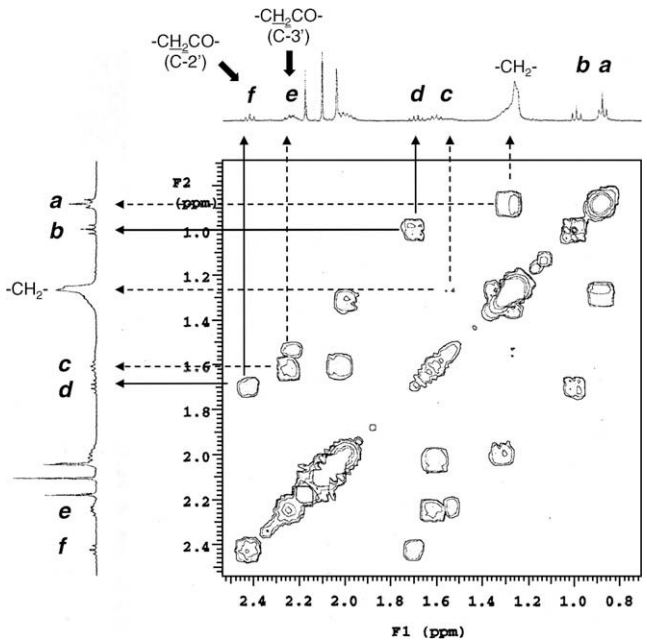


**Figure 6.** $^{1}H$–$^{1}H$ COSY spectrum of GL-A produced by *P. crassa*.

We further investigated the fatty acid profile of GL-A produced from oleic acid. The fatty acids at the C-3′ position of GL-A were composed mostly of $C_{14}$ or $C_{16}$ acids (Table 1), while those of MEL-A produced from soybean oils by *P. antarctica* were of $C_{10}$ acids. Based on all the above results, GL-A, the major product of *P. crassa*, was identified as a mixture of 4-*O*-[(2′,4′,6′-tri-*O*-acetyl-3′-*O*-alka(e)noyl-β-D-mannopyranosyl]-(2*R*,3*S*)-erythritol and 4-*O*-[(4′,6′-di-*O*-acetyl-3′-*O*-alka(e)noyl-2′-*O*-butanoyl)-β-D-mannopyranosyl]-(2*R*,3*S*)-erythritol as shown in Figure 7. The molecular weight of GL-A was 641.8 (acetic and $C_{14:1}$ acids) or 669.8 (butanoic and $C_{14:1}$ acids), which was determined from the main peak ($[M+Na]^+$) on matrix-assisted laser desorption/ionization time-of-flight mass spectrometry (MALDI-TOFMS) analysis; this is well consistent with the above structure.

**Table 1**
The fatty acid profiles of GL-A

| Fatty acid | GL-A |
|---|---|
| 12:0 | – |
| 14:0 | 12.2 |
| 14:1 | 53.0 |
| 16:0 | 4.6 |
| 16:1 | 19.0 |
| 18:0 | – |
| 18:1 | 3.1 |
| Unknown | 8.1 |

The structural determination of GL-B and GL-C was performed in a manner similar to that described above. Both have structures similar to that of GL-A except for the absence of an acetyl group at the C-4′ or C-6′ position. GL-B did not possess an acetyl group at the C-4′ position, and was identified as a new diastereomer of conventional MEL-B. GL-C without an acetyl group at the C-6′ position was also identified as a new diastereomer of conventional MEL-C.

### 2.3. Interfacial and biochemical properties of GL-A produced by *P. crassa* CBS 9959$^{T}$

In comparison with the structure of the conventional MEL-A produced by *P. antarctica*, that of GL-A was greatly different both in the hydrophilic and hydrophobic parts. Therefore, we expected that GL-A would show different glycolipid functions from those of conventional MEL-A. We thus partially examined the interfacial and biochemical properties of GL-A produced from oleic acids, such as surface-active properties, lyotropic liquid crystal formation, and immunoglobulin binding. In these experiments, MEL-A was also used as a reference.

#### 2.3.1. Surface-active properties of GL-A

We determined the surface tension of GL-A by the Wilhelmy method. Figure 8 shows the surface (air–water) tension versus concentration plot of GL-A in distilled water. The estimated critical micelle concentration (CMC) and surface tension at the CMC ($\gamma$CMC) were $5.2 \times 10^{-6}$ M and 26.5 mN/m, respectively. The occupation area of a molecule of GL-A at the surface was 43 Å$^2$/molecule. On the other hand, those of MEL-A were $2.7 \times 10^{-6}$ M, 28.4 mN/m, 60 Å$^2$/molecule, respectively. As expected, GL-A showed a slightly higher CMC and hydrophilicity compared to MEL-A, retaining an excellent surface-tension lowering activity. Indeed, on TLC analysis, the three glycolipids produced by *P. crassa* showed lower $R_f$ values and higher hydrophilicity than

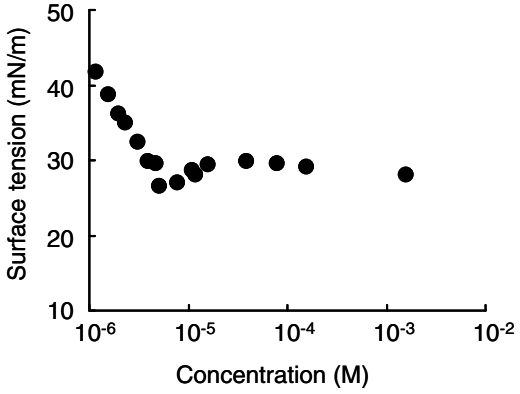


**Figure 8.** Surface tension–concentration plot of GL-A produced by *P. crassa* at 25 °C.

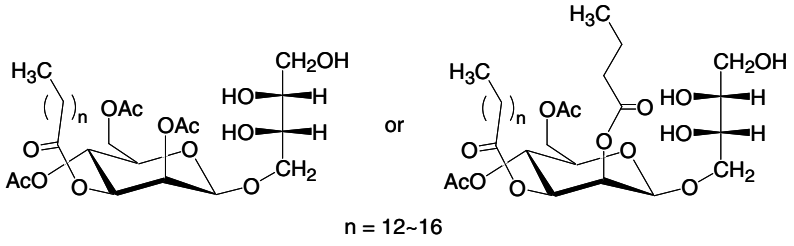


**Figure 7.** The presumable structures of GL-A produced by *P. crassa*.

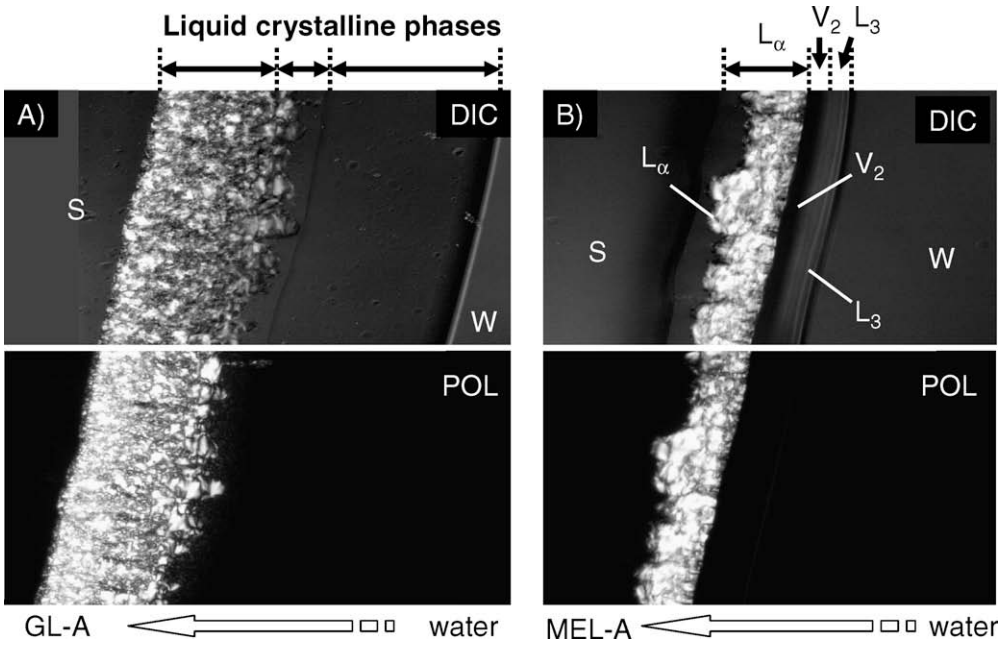


**Figure 9.** Water penetration scans of: (A) GL-A produced by *P. crassa* and (B) MEL-A produced by *P. antarctica*, viewed with and without crossed-polarizing filters. DIC: differential interference contrast microscopy; POL: polarized microscopy.

conventional MEL-A, -B, and -C. The significant difference in the occupation area between GL-A and MEL-A is probably due to the difference in the chain-length of fatty acyl group at the C-2′ position on the mannose moiety.

### 2.3.2. Formation of lyotropic liquid crystals

We also tentatively investigated the aqueous phase behavior of GL-A. The difference in the self-assembling manner between GL-A and conventional MEL-A would cause the difference in the lyotropic liquid crystalline structure. To observe the formation of liquid crystalline phases, the water-penetration method was performed as previously reported.[18]

Figures 9A and B show photographs for GL-A and MEL-A with increasing concentration from right to left, respectively. These photographs were viewed with (lower, POL) and without (upper, DIC) crossed-polarizing filters. On the basis of our previous phase study on conventional MELs,[18] the photographs should indicate several different regions that represent water (W), three or more crystal phases such as sponge ($L_3$), bicontinuous cubic ($V_2$), lamella ($L_\alpha$), and the neat surfactant phase (S). These results clearly demonstrated that the aqueous phase behavior of GL-A is significantly different from that of MEL-A.

### 2.3.3. Affinity binding toward immunoglobulins

We previously demonstrated that the self-assembled monolayer (SAM) of MEL-A shows high binding affinity toward different immunoglobulins such as human immunoglobulin G (HIgG), A (HIgA), and M (HIgM) through the 'multivalent' and 'carbohydrate-protein interactions'.[13,14] This activity seems to be greatly affected by the carbohydrate structure, especially by the orientation and/or configuration of the sugar moiety. For example, SAMs of MEL-B and -C show little binding affinity toward HIgG.[14] Therefore, we examined the interaction between the SAM of GL-A and HIgG by surface plasmon resonance (SPR) spectroscopy as previously reported.

Figure 10 shows SPR sensorgrams for binding of HIgG toward SAMs of GL-A and MEL-A. The response unit (RU) is a unit that shows the amounts of bound analytes (IgG) to the glycolipid

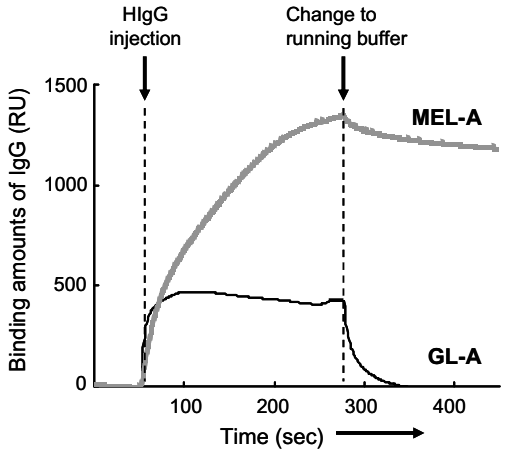


**Figure 10.** SPR sensorgrams for binding of HIgG toward SAMs of GL-A and MEL-A.

SAM, and 1000 RU corresponds to 1 ng of protein.[26] Interestingly, the SAM of GL-A showed no binding affinity to HIgG. This may be due to the difference in the surface structure of the SAM between the two glycolipids, which is derived from the difference in the molecular structure and/or self-assembling manner.

Accordingly, the present glycolipid that is the diastereomer of conventional MEL-A should provide us with different glycolipid functions, and thus facilitate a broad range of applications of MELs.

## 3. Discussion

The present structural analyses demonstrated that the glycolipids produced from oleic acids by *P. crassa* are MELs, but have a different chirality on the carbohydrate moiety compared to conventional MEL-A, -B, and -C. They were identified as 4′- and/or 6′-*O*-acetylated 4-*O*-(2′,3′-di-*O*-alka(e)noyl-β-D-mannopyranosyl)-(2*R*,3*S*)-erythritol, in which the erythritol configuration is entirely opposite to that of known MELs.

In NMR analysis, the coupling constant generally has a close relation to the stereochemistry of the molecular structure. As expected, the coupling constants of H-4a ($J$ = 5.2, 11.2 Hz) and 4b ($J$ = 3.6, 11.2 Hz) of GL-A were similar to those of the MEL-A diastereomer previously synthesized by Crich et al.[24] However, in the case of these glycolipids, the coupling constants of H-4 were almost same between two MEL-A diastereomers despite their different configuration.[24] This might be due to the intramolecular hydrogen bonding derived from the specific carbohydrate structure unlike a linear polyol. Therefore, with only these results, it seems very difficult to discuss the relationship between the stereochemistry and the coupling constants.

Very recently, we have found that *P. tsukubaensis* efficiently produces 4-*O*-(6′-*O*-acetyl-2′,3′-di-*O*-alka(e)noyl-β-D-mannopyranosyl)-(2*R*,3*S*)-erythritol, which is a diastereomer of conventional MEL-B.[25] In fact, partial $^1$H NMR spectrum of the carbohydrate moiety of GL-B produced by *P. crassa* completely corresponded with that of the novel MEL-B produced by *P. tsukubaensis*. Therefore, both *P. crassa* and *P. tsukubaensis* are speculated to possess a different mannosyltransferase from other *Pseudozyma* yeasts to give the unique carbohydrate configuration.

It should be noted that *P. crassa* is able to provide us with all diastereomers corresponding to conventional MEL-A, -B, and -C, although *P. tsukubaensis* gives only the MEL-B diastereomer. Obviously, the present basidiomycetous yeast has great potential as a novel MEL producer, although the glycolipid yield should be improved by further investigation on the culture conditions.

Another interesting feature of the present glycolipids is the unique hydrophobic part, which is substantially different from conventional MELs that comprise two medium-chain acids. The present glycolipids possessed a short chain (an acetyl or a butanoyl group) at the C-2′ position and a long chain ($C_{14}$, $C_{16}$, or $C_{18}$ acid) at the C-3′ position of the mannose moiety. They may thus act as a 'single chain surfactant' at the air-water surface, while conventional MELs do as 'double chain surfactant'. Indeed, the observed occupation area of a molecule of GL-A (43 Å$^2$/molecule) at the surface was much smaller than that of MEL-A (60 Å$^2$/molecule). In addition, on TLC, GL-A, -B, and -C showed lower $R_f$ values than those of MEL-A, -B, and -C, respectively (Fig. 3). Taking these facts into consideration, the present diastereomers would have higher hydrophilicity and/or water-solubility compared to conventional MELs, and are highly advantageous for use as oil-in-water type emulsions, water-based moisturizers, and/or washing detergents. This is supported from the fact that the present ME is highly hygroscopic compared to conventional one.

Based on our previous study,[27] most of the fatty acids in conventional MELs produced are not de novo synthesized fatty acids, but are rather direct β-oxidation intermediates of the fatty acids employed as the carbon source. In the present study, the long chain fatty acids at the C-3′ position of the mannose moiety were mainly composed of mono-unsaturated acids such as $C_{14:1}$ and $C_{16:1}$ when oleic acid ($C_{18:1}$) was used as the main carbon source. Thus, these acids in GL-A should be the β-oxidation intermediates of oleic acids. On the other hand, the short alkyl ($C_2$ or $C_4$) chains at the C-2′ position are presumably synthesized via a different metabolic pathway. Absence of long-chain acids at the C-2′ position as well as absence of short-chain acids at the C-3′ position implies that *P. crassa* generates the present glycolipids by catalysis of two regioselective acyltransferases. Hewald et al. recently reported that *Ustilago maydis*, another MEL producer, has two different acyltransferases (Mac1 and Mac2), and they are independently responsible for acylation of hydroxyl groups at the C-2′ and C-3′ positions.[28] Further investigation of biosynthesis of these glycolipids will provide us much useful information on the development of various glycolipid biosurfactants.

As mentioned above, the glycolipids produced by *P. crassa* have unprecedented molecular structures. Interestingly, the CMC and γCMC values of GL-A ($5.2 \times 10^{-6}$ M and 26.5 mN/m) were comparable to those of conventional MEL-A, although GL-A would have higher hydrophilicity than MEL-A as indicated above. We previously reported that the mono-acylated MEL bearing a long-chain acid at the C-3′ position showed more than 100-fold higher CMC value ($3.6 \times 10^{-4}$ M) than that of conventional di-acylated MELs.[29] The γCMC value (34 mN/m) of the mono-acylated was higher compared to those of conventional MELs. Considering these results, the presence of fatty-acyl groups at the C-2′ and C-3′ positions should play an important role for generating high surface activity, whereas the carbohydrate chirality and chain length of the hydrophobic part may have little influence on the surface activity.

In the water penetration experiments, MEL-A was estimated to give three crystalline phases such as $L_3$ (sponge), $V_2$ (bicontinuous cubic), and $L_\alpha$ (lamella), in addition to water and neat surfactant phases. Formation of these three phases is supported by our previous results with small-angle-X ray scattering (SAXS).[19] On the other hand, GL-A was estimated to show three different phases other than water and neat surfactant phases. The major optically anisotropic phase could be $L_\alpha$ (lamella) phase, considering the clear reflection pattern with crossed-polarizers. This $L_\alpha$ phase was also estimated to contain a different optically anisotropic phase that showed a little different reflection pattern from the left side of $L_\alpha$ phase. In addition, there may be one more optically isotropic phase, which shows no reflection with crossed-polarizers, between $L_\alpha$ and water phases. Further characterization should be done to clarify the structures of these crystalline phases.

In SPR experiments, the SAM of GL-A did not show any binding affinity toward IgG unlike that of MEL-A. Generally, the configuration of hydroxyl groups on the carbohydrate moiety plays an important role in the molecular recognition between proteins and carbohydrates.[30] It seems reasonable that conventional MEL-A shows high binding affinity toward IgG, while GL-A as a diastereomer of MEL-A does not, considering the distinctive difference in the configuration of erythritol between the glycolipids. Further investigation on the phase behavior and biological activity of the present glycolipids is underway; this would provide us with useful information on the structure–function relationship of glycolipid biosurfactants.

## 4. Conclusion

*P. crassa* produced new types of glycolipid biosurfactants from soybean oils or oleic acids. Their structures were identified as 4′- and/or 6′-*O*-acetylated 4-*O*-(2′-*O*-acetyl or butanoyl-3′-*O*-alka(e)noyl-β-D-mannopyranosyl)-(2*R*,3*S*)-erythritol. Thus, they were the diastereomers of known MELs, namely MEL-A, -B, and -C. GL-A, the major component of the diastereomers, showed nearly the same excellent surface active properties as the conventional MEL-A, although it exhibited different aqueous phase behavior and biochemical properties. They should thus show different glycolipid functions from those of MELs hitherto reported. This study will expand the variety of glycolipid biosurfactants and advance the research and development of them.

## 5. Experimental

### 5.1. Materials and microorganisms

All reagents and solvents were commercially available and were used as received. *P. crassa* CBS 9959$^T$ was obtained from Centraalbureau voor Schimmelcultures, the Netherlands. *P. antarctica* T-34, which was isolated from the exudates of a tree, was also used as a

MEL producer.[31] Stock cultures were cultivated for three days at 25 °C on an agar medium containing 4% glucose, 0.3% $NaNO_3$, 0.03% $MgSO_4$, 0.03% $KH_2PO_4$, and 0.1% yeast extract. They were stored at 4 °C and renewed every two weeks.

### 5.2. Molecular phylogenetic analysis

The sequences of internal transcribed spacer 1 (ITS1), 5.8S rRNA gene, and internal transcribed spacer 2 (ITS2) of each yeast strain were obtained from the DNA Data Bank of Japan (DDBJ) (http://www.ddbj.nig.ac.jp) and aligned using CLUSTAL W software.[32] The phylogenetic tree was visualized by TREEVIEW software (http://taxonomy.zoology.gla.ac.uk/rod/treeview.html).

### 5.3. General methods of the production and isolation of glycolipids

The following standard procedure for the production of glycolipids (MELs) was adopted. Seed cultures were prepared by inoculating cells grown on slants into test tubes containing a growth medium [4% glucose, 0.3% $NaNO_3$, 0.03% $MgSO_4$, 0.03% $KH_2PO_4$, 0.1% yeast extract (pH 6.0)] at 25 °C on a reciprocal shaker (200 strokes/min) for two days.

Seed cultures (1 mL) were transferred to 300 mL Erlenmeyer flasks containing 30 mL of a basal medium [4% soybean oil, 0.3% $NaNO_3$, 0.03% $MgSO_4$, 0.03% $KH_2PO_4$, 0.1% yeast extract (pH 6.0)], and then incubated on a rotary shaker (200 rpm) at 25 °C for 7 days, unless otherwise indicated.

Large-scale production of glycolipids was carried out at 25 °C for 7 days, stirred at 600 rpm, and aerated at a rate of 1.0 vvm in a jar fermentor (5.0 L) (B. E. Marubishi, Co. Ltd, Tokyo, Japan) containing 3.0 L of a fermentation medium [4% glucose, 4% oleic acid, 0.3% $NaNO_3$, 0.03% $MgSO_4$, 0.03% $KH_2PO_4$, 0.1% yeast extract (pH 6.0)]. Seed cultures were prepared with the growth medium as described above, and inoculated at 5% (v/v) to start the fermentation.

The produced glycolipids were extracted from the culture medium with an equal volume of EtOAc. The extracts were analyzed by TLC on silica plates (Silica Gel 60F; Wako) with a solvent system consisting of $CHCl_3$–MeOH–7 M aq $NH_3$ (65:15:2, by vol). The compounds on the plates were located by charring at 110 °C for 5 min after spraying an anthrone/sulfuric acid reagent as previously reported.[31] The purified MEL fraction including MEL-A, -B, and -C prepared as reported previously[33] was used as a standard.

The above organic layer was separated and evaporated. The concentrated glycolipids were dissolved in $CHCl_3$ and then purified by silica gel (Wako-Gel C-200) column chromatography using a gradient elution of $CHCl_3$–acetone (10:0→0:10, vol/vol) mixtures as solvent systems.[31,33] The purified glycolipids, namely GL-A, -B, and -C, were used in the following experiments.

#### 5.3.1. GL-A

$R_f$ = 0.57 ($CHCl_3$–MeOH–7 M aq $NH_3$ 65:15:2); $^1$H NMR ($CDCl_3$, 400 MHz): $\delta$ 5.50 (d, 1H, $J$ = 4 Hz, H-2′), 5.24–5.44 (b, 1.8H, –CH=CH–), 5.25 (t, 1H, $J$ = 10 Hz, H-4′), 5.08 (dd, 1H, $J$ = 3.2, 10 Hz, H-3′), 4.74 (s, 1H, H-1′), 4.23 (m, 2H, H-6′), 3.96 (dd, 1H, $J$ = 3.6, 11.2 Hz, H-4b), 3.91 (dd, 1H, $J$ = 5.2, 11.2 Hz, H-4a), 3.79 (m, 1H, H-3), 3.74–3.78 (m, 2H, H-1), 3.72 (m, 1H, H-5′), 3.67 (m, 1H, H-2), 2.42 (t, 0.8H, $J$ = 7.2 Hz, –$CH_2$C=O at the C-2′ position), 2.24 (m, 2H, –$CH_2$C=O at the C-3′ position), 2.18 (s, 1.9H, Ac at the C-2′ position), 2.10 (s, 3H, Ac at the C-6′ position), 2.04 (s, 3H, Ac at the C-4′ position), 1.94–2.06 (b, 3.6H, –C$H_2$CH=CH–), 1.64 (sextet, 0.8H, $J$ = 3.2 Hz, $CH_3CH_2CH_2$C=O at the C-2′ position), 1.50–1.64 (b, 2H, –C$H_2CH_2$C=O at the C-3′ position), 1.22–1.38 (b, 16H, –$CH_2$–), 0.99 (t, 1.2H, $J$ = 7.6 Hz, C$H_3CH_2CH_2$C=O at the C-2′ position), 0.88 (m, 3H, $CH_3$ of a fatty acid at the C-3′ position); $^{13}$C NMR ($CDCl_3$, 100 MHz): $\delta$ 173.4 (RC=O at the C-2′ position), 172.8 (RC=O at the C-3′ position), 170.9 (C=O(Ac) at the C-6′ position), 170.8 (C=O(Ac) at the C-2′ position), 169.8 (C=O(Ac) at the C-4′ position), 131.6 and 128.1 (–CH=CH–), 99.3 (C-1′), 72.7 (C-5′), 72.6 (C-4), 72.0 (C-2), 71.6 (C-3), 70.8 (C-3′), 69.0 and 68.8 (C-2′), 66.2 (C-4′), 63.9 (C-1), 62.6 (C-6′), 36.2 (–C$H_2$C=O at the C-2′ position), 33.7 (–C$H_2$C=O at the C-3′ position), 32.1, 29.5-29.9, and 22.9 (–$CH_2$–), 27.5 and 26.6 (–C$H_2$CH=CH–), 24.9 (–C$H_2CH_2$C=O at the C-3′ position), 21.0 ($CH_3$(Ac) at the C-2′ position), 20.9 × 2 ($CH_3$(Ac) at the C-4′ and C-6′ position), 18.8 ($CH_3CH_2CH_2$C=O at the C-2′ position), 14.3 ($CH_3$ of a fatty acid at the C-3′ position), 13.8 ($CH_3CH_2CH_2$C=O at the C-2′ position).

#### 5.3.2. GL-B

$R_f$ = 0.49 ($CHCl_3$–MeOH–7 M aq $NH_3$ 65:15:2); $^1$H NMR ($CDCl_3$, 400 MHz): $\delta$ 5.49 (d, 1H, $J$ = 2.8 Hz, H-2′), 5.25–5.45 (b, 2H, –CH=CH–), 4.92 (dd, 1H, $J$ = 3.2, 10 Hz, H-3′), 4.74 (s, 1H, H-1′), 4.44 (m, 2H, H-6′), 3.94 (dd, 1H, $J$ = 3.6, 10.8 Hz, H-4b), 3.89 (dd, 1H, $J$ = 5.6, 10.8 Hz, H-4a), 3.80 (m, 1H, H-4′), 3.75 (m, 1H, H-6′), 3.70–3.82 (m, 3H, H-1 and H-3), 3.65 (m, 1H, H-2), 3.59 (m, 1H, H-5′), 2.39 (t, 0.2H, $J$ = 7.2 Hz, –$CH_2$C=O at the C-2′ position), 2.31 (m, 2H, –$CH_2$C=O at the C-3′ position), 2.15 (s, 2.8H, Ac at the C-2′ position), 2.14 (s, 3H, Ac at the C-6′ position), 1.94–2.08 (b, 4H, –C$H_2$CH=CH–), 1.55–1.72 (b, 2.2H, –C$H_2CH_2$C=O), 1.22–1.38 (b, 16H, –$CH_2$–), 0.99 (t, 0.3H, $J$ = 7.6 Hz, C$H_3CH_2CH_2$C=O at the C-2′ position), 0.88 (m, 3H, $CH_3$ of a fatty acid at the C-3′ position); $^{13}$C NMR ($CDCl_3$, 100 MHz): $\delta$ 173.7 (RC=O), 171.8 (C=O(Ac) at the C-6′ position), 170.7 (C=O(Ac) at the C-2′ position), 129.5–131.6 (–CH=CH–), 99.4 (C-1′), 74.8 (C-5′), 73.3 (C-3′), 72.5 (C-4), 72.1 (C-2), 71.7 (C-3), 69.2 (C-2′), 65.8 (C-4′), 63.9 (C-1), 63.4 (C-6′), 33.7–34.3 (–C$H_2$C=O at the C-3′ position), 32.1, 29.5–29.9, and 22.9 (–$CH_2$–), 26.7–27.5 (–C$H_2$CH=CH–), 24.8 (–C$H_2CH_2$C=O at the C-3′ position), 21.0 × 2 ($CH_3$(Ac) at the C-2′ and C-6′ position), 14.3 ($CH_3$).

#### 5.3.3. GL-C

$R_f$ = 0.39 ($CHCl_3$–MeOH–7 M aq $NH_3$ 65:15:2); $^1$H NMR ($CDCl_3$, 400 MHz): $\delta$ 5.49 (d, 1H, $J$ = 2.4 Hz, H-2′), 5.24–5.44 (b, 2H, –CH=CH–), 5.17 (t, 1H, $J$ = 10 Hz, H-4′), 5.10 (dd, 1H, $J$ = 3.2, 10 Hz, H-3′), 4.77 (s, 1H, H-1′), 3.97 (dd, 1H, $J$ = 5.2, 11.2 Hz, H-4b), 3.90 (dd, 1H, $J$ = 3.2, 11.2 Hz, H-4a), 3.70–3.82 (m, 4H, H-1, H-2, and H-3), 3.68 (m, 2H, H-6′), 3.55 (m, 1H, H-5′), 2.41 (t, 0.2H, $J$ = 7.2 Hz, –$CH_2$C=O at the C-2′ position), 2.24 (t, 2H, $J$ = 7.6 Hz, –$CH_2$C=O at the C-3′ position), 2.17 (s, 2.7H, Ac at the C-2′ position), 2.05 (s, 3H, Ac at the C-4′ position), 1.94–2.06 (b, 4H, –C$H_2$CH=CH–), 1.68 (sextet, 0.2H, $J$ = 7.6 Hz, $CH_3CH_2CH_2$C=O at the C-2′ position), 1.50–1.64 (b, 2H, –C$H_2CH_2$C=O at the C-3′ position), 1.22–1.38 (b, 19H, –$CH_2$–), 0.98 (t, 0.2H, $J$ = 7.2 Hz, C$H_3CH_2CH_2$C=O at the C-2′ position), 0.88 (t, 3H, $J$ = 6.8 Hz, $CH_3$ of a fatty acid at the C-3′ position); $^{13}$C NMR ($CDCl_3$, 100 MHz): $\delta$ 173.3 (RC=O), 170.8 (C=O(Ac) at the C-2′ position), 170.4 (C=O(Ac) at the C-4′ position), 130.5 and 129.5 (–CH=CH–), 99.1 (C-1′), 75.1 (C-5′), 72.1 (C-4), 72.0 (C-2), 71.4 (C-3), 70.8 (C-3′), 69.2 (C-2′), 66.4 (C-4′), 63.7 (C-1), 61.5 (C-6′), 34.3 (–$CH_2$C=O at the C-3′ position), 32.1, 29.5–30.0, and 22.9 (–$CH_2$–), 27.5 and 27.2 (–C$H_2$CH=CH–), 24.9 (–C$H_2CH_2$C=O at the C-3′ position), 21.0 ($CH_3$(Ac) at the C-2′ position), 20.9 ($CH_3$(Ac) at the C-4′position), 14.3 ($CH_3$).

### 5.4. Preparation of mannosylerythritol by alkaline hydrolysis of glycolipids

The glycoside (mannosylerythritol, ME) was prepared by alkaline hydrolysis of glycolipids as previously reported.[25] To a solution of the mixture of glycolipids (680 mg, 1 mmol) in dry MeOH (5 mL) was added NaOMe (20 mg, 370 μmol) in dry MeOH (5 mL). In

addition to the mixture of glycolipids obtained with *P. crassa*, we also used the mixture obtained with *P. antarctica* as a reference. After stirring at room temperature for 1 h, cation exchange resin (DOWEX H+ form, >1 g) was added and the reaction mixture was stirred further. After stirring for 15 min, the resin was removed by filtration, and the filtrate was evaporated. To the residue was added a small amount of water (1 mL) and EtOAc (10 mL), then the fatty acids were extracted with EtOAc. The resulting aqueous layer containing the sugar moiety was concentrated to a syrup. Purification of the glycoside (ME) was performed by recrystallization from 90% ethanol. ME from *P. antarctica* was obtained (224 mg, 0.79 mmol) as a white needle crystal, and that from *P. crassa* was obtained (250 mg, 0.88 mmol) as a colorless syrup.

#### 5.4.1. ME from *P. crassa* (4-*O*-β-D-mannopyranosyl-(2*R*,3*S*)-erythritol)

$[\alpha]_D^{27}$ −41.9 (*c* 1.0, $H_2O$); $^1H$ NMR ($D_2O$, 400 MHz): $\delta$ 4.55 (d, 1H, *J* = 0.4 Hz, H-1′), 3.88 (dd, 1H, *J* = 0.8, 3.2 Hz, H-2′), 3.84 (dd, 1H, *J* = 5.6, 11.2 Hz, H-4b), 3.78 (dd, 1H, *J* = 2.4, 12 Hz, H-6′b), 3.71 (dd, 1H, *J* = 2.8, 11.2 Hz, H-4a), 3.66 (dd, 1H, *J* = 2.4, 6.4 Hz, H-1b), 3.63 (m, 1H, H-2), 3.61 (m, 1H, H-3), 3.58 (m, 1H, H-6′a), 3.51 (m, 1H, H-3′), 3.48 (m, 1H, H-1a), 3.42 (t, 1H, *J* = 9.6 Hz, H-4′), 3.23 (m, 1H, H-5′); $^{13}C$ NMR ($D_2O$, 100 MHz): $\delta$ 100.1 (C-1′), 76.4 (C-5′), 73.0 (C-3′), 71.7 (C-3), 70.7 (C-2), 70.4 x2 (C-2′ and C-4), 67.0 (C-4′), 62.7 (C-1), 61.2 (C-6′).

#### 5.4.2. ME from *P. antarctica* (4-*O*-β-D-mannopyranosyl-(2*S*,3*R*)-erythritol)

Mp 155.4–158.3 °C; $[\alpha]_D^{26}$ −35.2 (*c* 1.0, $H_2O$); $^1H$ NMR ($D_2O$, 400 MHz): $\delta$ 4.54 (d, 1H, *J* = 0.4 Hz, H-1′), 3.92 (dd, 1H, *J* = 2.4, 10.8 Hz, H-4b), 3.89 (d, 1H, *J* = 2.8 Hz, H-2′), 3.77 (dd, 1H, *J* = 2.4, 12.4 Hz, H-6′b), 3.67 (dd, 1H, *J* = 2.4, 6.4 Hz, H-1b), 3.64 (dd, 1H, *J* = 2.8, 11.2 Hz, H-4a), 3.60 (m, 1H, H-2), 3.58 (m, 1H, H-3), 3.56 (m, 1H, H-6′a), 3.50 (m, 1H, H-3′), 3.48 (m, 1H, H-1a), 3.41 (t, 1H, *J* = 9.6 Hz, H-4′), 3.23 (m, 1H, H-5′); $^{13}C$ NMR ($D_2O$, 100 MHz): $\delta$ 100.6 (C-1′), 76.4 (C-5′), 73.0 (C-3′), 71.9 (C-3), 70.8 (C-4), 70.7 (C-2), 70.6 (C-2′), 67.0 (C-4′), 62.7 (C-1), 61.2 (C-6′).

### 5.5. Structure determination of the purified glycolipids

Structure determination of the purified glycolipids and glycosides dissolved in $CDCl_3$ or $D_2O$ was performed by $^1H$, $^{13}C$ NMR, and two-dimensional NMR analysis, such as $^1H$–$^1H$ COSY, HMQC, and HMBC using a Varian INOVA 400 (400 MHz). Specific rotations of glycosides were measured by JASCO Digital Polarimeter DIP-370 in aqueous solution. The molecular weights of the purified glycolipids were measured by MALDI-TOF/MS (Voyager-DE PRO) with an α-cyano-4-hydroxycinnamic acid matrix. The fatty acid profiles of the purified glycolipids were examined by gas chromatography–mass spectrometry (GC–MS) as previously reported.[6] The methyl ester derivatives of fatty acids were prepared by mixing the above purified glycolipids (10 mg) with 5% HCl–MeOH reagent (1 mL) (Tokyo Kasei Kogyo, Tokyo, Japan) at 80 °C for 20 min. After the reaction mixture was quenched with water (1 mL), the methyl ester derivatives were extracted with *n*-hexane and then analyzed by GC-MS (Hewlett Packard 6890 and 5973N) with a TC-WAX (GL-science, Tokyo) with the temperature programmed from 90 °C (held for 3 min) to 240 °C at 5 °C/min.

### 5.6. Determination of surface tension of the purified glycolipid

Surface tension of the purified glycolipid (GL-A) was determined by a Wilhelmy-type automatic tensionmeter CBVP-A3 (Kyowa-kaimenkagaku, Tokyo, Japan) at 25 °C. Occupation area of the molecule at the air–water surface was calculated from surface excess concentration with Gibbs adsorption equation by the method previously reported.[34]

### 5.7. Water penetration scan technique

To examine the lyotropic liquid crystalline phase behavior of the purified glycolipids (GL-A and MEL-A), the water penetration scan method was used as previously reported.[18] A polarized optical microscope (ECLIPSE E-600, Nikon, Japan) with crossed-polarizing filters equipped with a charge-coupled-device camera (DS-SM, Nikon) was used for the scan. Birefringent textures from the optical microscopy allowed the assignment of the particular lyotropic phase types to the samples.

### 5.8. Surface plasmon resonance spectroscopy

To investigate the interaction between the self-assembled monolayer (SAM) of the purified glycolipid and human immunoglobulin (HIgG), surface plasmon resonance (SPR) measurement was performed with a BIAcore X instrument (BIAcore, Inc.) using HPA sensor chips. All experiments were done at 25 °C. The running buffer (10 mM HEPES, 150 mM NaCl, pH 7.4) was freshly prepared and degassed by sonication for 30 min. After the HPA chip was installed, the alkanethiol surface was cleaned with sodium dodecyl sulfate (SDS) (0.5% (w/v), 20 μL) at a flow rate of 20 μL/min. GL-A or MEL-A bilayer membrane (0.5 mM, 25 μL) was prepared and filtered through 100 nm pores as previously reported,[14] and was then applied to the chip surface at a low flow rate of 5 μL/min. To confirm complete coverage of the glycolipid layer, HSA (350 nM, 75 μL) was injected at a flow rate of 20 μL/min. The lyophilized HIgG (Sigma) was dissolved in buffer (10 mM HEPES, 150 mM NaCl, pH 7.4), and the obtained solutions (350 nM, 75 μL) were injected on the glycolipid surface at a flow rate of 20 μL/min.

SPR data were analyzed by the following procedure. Changes in the SPR angle, given in response units (RU), are proportional to the amount of protein in the immediate vicinity of the sensor chip surface and 1000 RU corresponds to 1 ng of protein.[26] The amounts of bound analytes were defined as RU at 400 s after the injection.

## Acknowledgments

We would like to thank Ms. Akiko Sugimura, a fellow of the Japan Industrial Technology Association, for her technical assistance. This work was supported by the Industrial Technology Research Grant Program in 06A10571c from the New Energy and Industrial Technology Development Organization (NEDO) of Japan.

## References

1. Banat, I. M.; Makkar, R. S.; Cameotra, S. S. *Appl. Microbiol. Biotechnol.* **2000**, *53*, 495–508.
2. Kitamoto, D.; Isoda, H.; Nakahara, T. *J. Biosci. Bioeng.* **2002**, *94*, 187–201.
3. Lang, S. *Curr. Opin. Colloid Interface Sci.* **2002**, *7*, 12–20.
4. Kitamoto, D.; Ikegami, T.; Suzuki, T.; Sasaki, A.; Takeyama, Y.; Idemoto, Y.; Koura, N.; Yanagishita, H. *Biotechnol. Lett.* **2001**, *23*, 1709–1714.
5. Rau, U.; Nguyen, L. A.; Schulz, S.; Wray, V.; Nimtz, M.; Roper, H.; Koch, H.; Lang, S. *Appl. Microbial. Biotechnol.* **2005**, *66*, 551–559.
6. Morita, T.; Konishi, M.; Fukuoka, T.; Imura, T.; Kitamoto, D. *Appl. Microbiol. Biotechnol.* **2006**, *73*, 305–313.
7. Kitamoto, D.; Yanagishita, H.; Shinbo, T.; Nakane, T.; Kamisawa, C.; Nakahara, T. *J. Biotechnol.* **1993**, *29*, 91–96.
8. Im, J. H.; Ikegami, T.; Yanagishita, H.; Takeyama, Y.; Idemoto, Y.; Koura, N.; Kitamoto, D. *J. Biomed. Mater. Res.* **2003**, *65*, 379–385.
9. Inoh, Y.; Kitamoto, D.; Hirashima, N.; Nakanishi, M. *J. Control. Release* **2004**, *94*, 423–431.
10. Igarashi, S.; Hattori, Y.; Maitani, Y. *J. Control. Release* **2006**, *112*, 362–368.
11. Rodorigues, L.; Banat, I. M.; Teixeria, J.; Oliveira, R. *J. Antimicrob. Chemother.* **2006**, *57*, 609–618.
12. Konishi, M.; Imura, T.; Fukuoka, T.; Morita, T.; Kitamoto, D. *Biotechnol. Lett.* **2007**, *29*, 473–480.

13. Imura, T.; Ito, S.; Azumi, R.; Yanagishita, H.; Sakai, H.; Abe, M.; Kitamoto, D. *Biotechnol. Lett.* **2007**, *29*, 865–870.
14. Ito, S.; Imura, T.; Fukuoka, T.; Morita, T.; Sakai, H.; Abe, M.; Kitamoto, D. *Colloids Surf., B* **2007**, *58*, 165–171.
15. Ueno, Y.; Inoh, Y.; Furuno, T.; Hirashima, N.; Kitamoto, D.; Nakanishi, M. *J. Control. Release* **2007**, *123*, 247–253.
16. Imura, T.; Yanagishita, H.; Kitamoto, D. *J. Am. Chem. Soc.* **2004**, *126*, 10804–10805.
17. Imura, T.; Yanagishita, H.; Ohira, J.; Sakai, H.; Abe, M.; Kitamoto, D. *Colloids Surf., B* **2005**, *43*, 114–121.
18. Imura, T.; Ohta, N.; Inoue, K.; Yagi, H.; Negishi, H.; Yanagishita, H.; Kitamoto, D. *Chem. Eur. J.* **2006**, *12*, 2434–2440.
19. Imura, T.; Hikosaka, Y.; Worakitkanchanakul, W.; Sakai, H.; Abe, M.; Konishi, M.; Minamikawa, H.; Kitamoto, D. *Langmuir* **2007**, *23*, 1659–1663.
20. Worakitkanchanakul, W.; Imura, T.; Morita, T.; Fukuoka, T.; Sakai, H.; Abe, M.; Rujiravanit, R.; Chavadej, S.; Kitamoto, D. *Colloids Surf., B* **2008**, *65*, 106–112.
21. Morita, T.; Konishi, M.; Fukuoka, T.; Imura, T.; Kitamoto, H. K.; Kitamoto, D. *FEMS Yeast Res.* **2007**, *7*, 286–292.
22. Konishi, M.; Morita, T.; Fukuoka, T.; Imura, T.; Kakugawa, K.; Kitamoto, D. *Appl. Microbiol. Biotechnol.* **2007**, *75*, 521–531.
23. Konishi, M.; Morita, T.; Fukuoka, T.; Imura, T.; Kakugawa, K.; Kitamoto, D. *Appl. Microbiol. Biotechnol.* **2008**, *78*, 37–46.
24. Crich, D.; de la Mora, M. A.; Cruz, R. *Tetrahedron* **2002**, *58*, 35–44.
25. Fukuoka, T.; Morita, T.; Konishi, M.; Imura, T.; Kitamoto, D. *Carbohydr. Res.* **2008**, *343*, 555–560.
26. Stenberg, E.; Persson, B.; Roos, H.; Urbaniczky, C. *J. Colloid Interface Sci.* **1991**, *143*, 513–526.
27. Kitamoto, D.; Yanagishita, H.; Haraya, K.; Kitamoto, HK. *Biotechnol. Lett.* **1998**, *20*, 813–818.
28. Hewald, S.; Linne, U.; Scherer, M.; Marahiel, M. A.; Kämper, J.; Bölker, M. *Appl. Environ. Microbiol.* **2006**, *72*, 5469–5477.
29. Fukuoka, T.; Morita, T.; Konishi, M.; Imura, T.; Sakai, H.; Kitamoto, D. *Appl. Microbiol. Biotechnol.* **2007**, *76*, 801–810.
30. Lis, H.; Sharon, N. *Chem. Rev.* **1998**, *98*, 637–674.
31. Kitamoto, D.; Akiba, S.; Hioki, C.; Tabuchi, T. *Agric. Biol. Chem.* **1990**, *54*, 31–36.
32. Thompson, J. D.; Higgins, D. G.; Gibson, T. J. *Nucleic Acids Res.* **1994**, *22*, 4673–4680.
33. Kitamoto, D.; Ghosh, S.; Ourisson, G.; Nakatani, Y. *Chem. Commun.* **2000**, *10*, 861–862.
34. Kwan, C. C.; Rosen, M. J. *J. Phys. Chem.* **1980**, *84*, 547–551.